

Charged particle display

Sung Nae Cho*

*MEMS & Packaging Group, Samsung Advanced Institute of Technology,
Mt. 14-1 Nongseo-dong Giheung-gu, Yongin-si Gyeonggi-do, 446-712, South Korea*
(Dated: Prepared 14 August 2008)

An optical shutter based on charged particles is presented. The output light intensity of the proposed device has an intrinsic dependence on the interparticle spacing between charged particles, which can be controlled by varying voltages applied to the control electrodes. The interparticle spacing between charged particles can be varied continuously and this opens up the possibility of particle based displays with continuous grayscale.

PACS numbers: 47.45.-n, 51.35.+a

I. INTRODUCTION

The flexibility and bistability are the two key points in the next generation display technologies. The flexibility implies the display would be thin, lightweight, and ultimately paper like, meaning it would be cheap enough to be disposable. The bistability implies the technology would be ecologically friendly. In the bistable display, the image does not need to be refreshed until rewritten and, therefore, a low level of power consumption is expected for still images. Unfortunately, the bistability has no advantages in power savings over non-bistable technologies, such as liquid crystal displays (LCDs), plasma display panels (PDPs), and organic light emitting diodes displays (OLEDs), for motion pictures.

The display technologies based on particles are the most prominent candidates for a flexible and bistable displays. The earliest display based on particles dates back to 1970s when Ota filed for a patent (author?) [1]. Since then various particle-displays based on electrophoresis and electrowetting principles have emerged to form what is now referred to as “E-paper technologies” in industry (author?) [2, 3, 4, 5, 6]. In electrophoresis, particles are usually suspended in a fluid. Because the speed at which particles move inversely vary with fluid density, particle-displays based on electrophoresis have slow response time, typically on the order of 300 ms (author?) [7, 8, 9]. This makes motion pictures unsuitable for electrophoretic particle-displays. The issue of slow response time in electrophoretic particle-displays, however, has been resolved with the unveil of Quick Response Liquid Powder Display (QR-LPD) by Hattori et al. (author?) [10, 11, 12, 13]. The QR-LPD is distinguished from the rest of particle based displays in that it uses air as the particle carrying medium rather than fluid. Because the particles in QR-LPD move in air, its response time is at 0.2 ms, which is even faster than LCDs. The sub-millisecond response time makes QR-LPD the only candidate based on particle-display capable of handling motion pictures, and researches are being

conducted for particle-displays with air as the particle carrying medium (author?) [14].

Common to all particle-displays, regardless of air or fluid used as the particle carrying medium, is the lack of continuous grayscale. A high grayscale range is essential to quality displays. Without it, the images displayed on monitors would be dull (author?) [15]. The most well known E-paper technology, E-Ink, obtains different gray states through modulation of voltages supplied to the control electrodes. Because the voltage is modulated at a value lower than the saturation voltage, which is the voltage required to display either all black or all white for a simple black-and-white display, the displayed image would have intensity somewhere between that of completely black and completely white. This approach to achieve different gray states, however, is done at the cost of losing bistability. Since the pixel is being constantly modulated to sustain a gray state, the situation is equivalent to motion pictures and the power savings from bistability no longer applies to gray states. In this work, a display architecture based on charged particles is presented. Unlike the previous particle display technologies, the proposed device has potential to generate continuous grayscale levels without sacrificing the benefit of bistability.

II. CHARGED PARTICLE DISPLAY

A. Device structure

The cross-sectional schematic of an optical shutter based on charged particles of same polarity is illustrated in Fig. 1. In the figure, the two electrodes, where each is labeled top and bottom electrodes, constitute the control electrodes. Because the light must be transmitted through the control electrodes, the electrodes are chosen from optically transparent conductors. The chamber, wherein the particles reside, can be a vacuum, filled with noble gas, or filled with air. The metallic reflectors, which forms the lateral surface of the chamber, are electrically connected to one of the control electrodes. This make metallic reflectors not only to reflect light, but also function as to keep particles from aggregating to the lateral

*Electronic address: sungnae.cho@samsung.com

surface of chamber. The optically transparent passivation layer, which is treated on the inner surface of the chamber, functions to prevent charge transfer between particles and conductors.

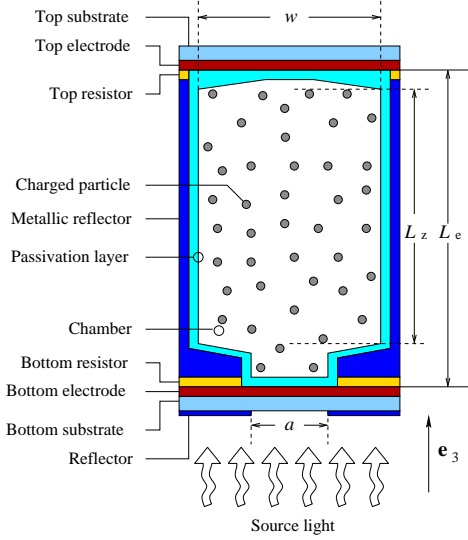


Figure 1: Transfective display based on charged particles.

B. Operation principle

The intensity of light transmitted through a medium filled with suspended spherical particles, illustrated in Fig. 2, is given by

$$I = I_0 \exp \left[-\frac{36n\pi k f h}{\lambda (n^2 + 2)^2} \right], \quad (1)$$

where n and k are respectively the real and imaginary part of the complex refractive index for the medium and the particles suspended in it; I_0 is the initial intensity, λ is the wavelength of light, h is the thickness of the volume containing charged particles, and f is the volume fraction of particles (author?) [16]. In explicit form, the volume fraction of particles is

$$f = \frac{N v_p}{A h},$$

where N is the total number of particles, v_p is the volume of a single particle, and A is the cross-sectional area illustrated in Fig. 2. Insertion of f into Eq. (1) gives

$$I = I_0 \underbrace{\exp \left[-\frac{36n\pi k v_p}{\lambda (n^2 + 2)^2} \right]}_C \exp \left(-\frac{N}{A} \right),$$

the terms enclosed in C is just a constant. The total number of particle in volume, N , can be separated into

those on and not on the cross-sectional area A illustrated in Fig. 2,

$$N = N_1 + N_2 \rightarrow \frac{N}{A} = \frac{N_1}{A} + \frac{N_2}{A},$$

where N_1 is the number of particles on A and N_2 is the number of particles not on A . The term N_1/A is identified with the average number of particles per unit cross-sectional area, where the particles constituting N_1 are indicated by the open circles in Fig. 2. Therefore, the intensity of light transmitted through a medium filled with suspended particles goes like

$$I \propto \exp(-\sigma_N), \quad \sigma_N = \frac{N_1}{A}, \quad (2)$$

where σ_N increases with volume compression. The fact that σ_N increases with compression of the volume containing particles is straightforward and this is illustrated in Fig. 2 for the compressed state. Throughout this work, I shall refer terms like “compressed state” or “compressed particle volume” to denote the compression of the volume containing particles as illustrated in Fig. 2.

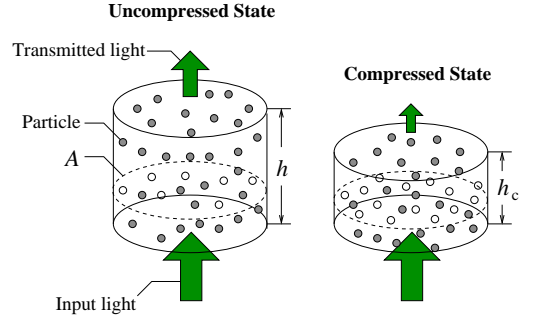


Figure 2: Transmission of light through a medium filled with total of N suspended spherical particles. Both compressed and uncompressed cases are shown. The open circles represent particles on the cross-sectional area, A .

The same principle which is inherent in Eq. (2) applies to the proposed optical shutter, Fig. 1. In the presented device, the chamber is filled with charged particles of same polarity and this can be identified with the medium filled with suspended particle in Fig. 2. The on set of electric field inside the chamber, which is done by controlling the voltage over one of the electrodes, causes particles to be compressed in volume, as illustrated in Fig. 3. Since the particles are assumed to be positively charged, they are compressed in the direction of electric field. Eventually, the compression comes to cease when particle-particle Coulomb repulsion counterbalances the compression induced by the control electrodes.

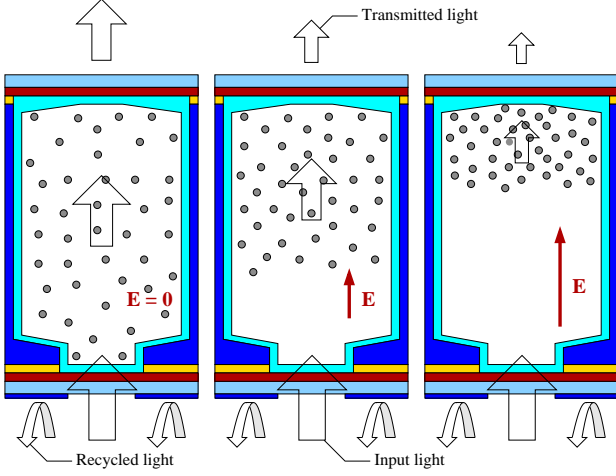


Figure 3: The on set of electric field compresses the filled volume for charged particles.

In principle, the level of compression for the particle volume can be varied continuously. Because the intensity of transmitted light varies with compression, i.e., Eq. (2), the display based on charged particles has potential to generate continuous gray levels. Also, since the control electrodes form a capacitor, provided there is no leakage (or negligible) current across the capacitor, the electric field inside the chamber can be sustained even when the device is disconnected from power. This opens up the possibility of a bistable mode for gray states as well.

To utilize charged particles in displays, a quantitative understanding of how design parameters, such as (L_e, L_z, ξ) for the sub-pixel dimensions and (r, ρ_m, Q) for the charged particle, enter into the compression mechanism is required. Here, r is the particle radius (assuming a spherical particle), ρ_m is the particle mass density, and Q is the net charge which the particle hold. Describing the compression mechanism in terms of design parameters is the task for the next section.

C. Theory

The optical shutter presented in this proposal relies on the density of particles in chamber to control the intensity of transmitted light. An analogy can be made to the driving under misty weather. When the density of water vapor suspended in the atmosphere is heavy, one is obscured in his or her viewing distance, as less light reaches the eye. Contrarily, the amount of light reaching the eye increases with a reduction in density of water vapor suspended in the atmosphere, thereby enabling the driver to see far distances.

The particles in chamber of the proposed optical shutter ranges in diameter anywhere from a few nanometers to several microns, assuming a spherical morphology. This range for the particle size, although small macroscopically, is much too large to be considered for a

treatment within quantum domain, where the quantum theory must be used for description. Therefore, the classical theory suffices for the description here. Since the charged particles in the system, as a whole, behave like a classical gas, the description is carried out in the realm of statistical physics.

To keep the topic presented here self-contained, I shall briefly summarize the kind of manipulations and approximations assumed in obtaining expressions which are considered crucial to the initial development of the analysis.

1. Maxwell-Boltzmann statistics

The charged particles in chamber can be treated as classical particles obeying the Maxwell-Boltzmann statistics (author?) [17]. The i th charged particle under influence of external forces, for example, gravitational and electric forces, assumes the energy

$$U_i = \frac{\mathbf{p}_i^2}{2m_i} + U_{\text{ext}} + U_{\text{int}}, \quad \mathbf{p}_i = \sum_j p_{ij} \mathbf{e}_j,$$

where \mathbf{p}_i is the center of mass momentum for the i th charged particle and the term associated with it is the kinetic energy, U_{ext} is the interaction energy with external influences, and U_{int} is the energy contribution arising only if the particle is not monatomic.

In explicit form, U_{ext} can be expressed as

$$U_{\text{ext}} = \sum_{j \neq i}^N \frac{k_q Q_i Q_j}{\left[(x_i - x_j)^2 + (y_i - y_j)^2 + (z_i - z_j)^2 \right]^{1/2}} + m_i g z_i + Q_i E z_i,$$

where N is the number of particles in volume, the Q_i and Q_j denote respectively the net charges for the i th and j th particles, E is the electric field magnitude, and the constants $g = 9.8 \text{ m s}^{-2}$ and $k_q = 8.99 \times 10^9 \text{ N m}^2 \text{ C}^{-2}$ in MKS system of units. For a monatomic particle, the energy contributions from the internal rotation and vibration with respect to its center of mass vanishes, $U_{\text{int}} = 0$. Therefore, the i th monatomic charged particle under the influence of external forces assumes the energy

$$U_i = \frac{\mathbf{p}_i^2}{2m_i} + m_i g z_i + Q E z_i + \sum_{j \neq i}^N \frac{k_q Q^2}{\left[(x_i - x_j)^2 + (y_i - y_j)^2 + (z_i - z_j)^2 \right]^{1/2}}, \quad (3)$$

where, for convenience, all particles in the system are assumed to be identically charged with same polarity, i.e., $Q_i = Q_j = Q$.

The gravity and electric field have directions, and this information must be taken into account in Eq. (3). To do this, the parameter z_i is first restricted to a domain

$$\{\mathcal{D} : 0 \leq z_i < \infty\}.$$

With z_i restricted to a domain defined by \mathcal{D} , the gravitational potential energy of a particle, $m_i g z_i$, increases with positive g and decreases with negative g as z_i increase. Therefore, the direction of gravity in Eq. (3) can be taken into account by

$$g = \begin{cases} +9.8 \text{ m s}^{-2} & \text{if gravity points in } -\mathbf{e}_3, \\ -9.8 \text{ m s}^{-2} & \text{if gravity points in } +\mathbf{e}_3. \end{cases} \quad (4)$$

The electric potential energy of a particle, $Q E z_i$, increases with positive E and decreases with negative E as z_i increase. For a positively charged particle, its electric potential energy increases as it moves against the direction of electric field and decreases as it moves in the direction of electric field. The direction of electric field inside the chamber can hence be taken into account in Eq. (3) by

$$E = \begin{cases} +E & \text{if } \mathbf{E} \text{ points in } -\mathbf{e}_3, \\ -E & \text{if } \mathbf{E} \text{ points in } +\mathbf{e}_3. \end{cases} \quad (5)$$

The probability of finding the particle with its center of mass position in the ranges $(\mathbf{R}_i; d\mathbf{R}_i)$ and $(\mathbf{p}_i; d\mathbf{p}_i)$ can be expressed as

$$P_s(\mathbf{R}_i, \mathbf{p}_i) d^3\mathbf{R}_i d^3\mathbf{p}_i \propto \exp\left(-\frac{U_i}{k_B T}\right) d^3\mathbf{R}_i d^3\mathbf{p}_i, \quad (6)$$

where T is the temperature in units of degree Kelvin ($^\circ\text{K}$) and k_B is the Boltzmann constant, $k_B = 1.38 \times 10^{-23} \text{ J}/(^\circ\text{K})$. With Eq. (3), $P_s(\mathbf{R}_i, \mathbf{p}_i) d^3\mathbf{R}_i d^3\mathbf{p}_i$ becomes

$$\begin{aligned} & P_s(\mathbf{R}_i, \mathbf{p}_i) d^3\mathbf{R}_i d^3\mathbf{p}_i \\ & \propto \exp\left(-\frac{\mathbf{p}_i^2}{2m_i k_B T}\right) d^3\mathbf{p}_i \\ & \times \exp\left(\sum_{j \neq i}^N \frac{-k_q k_B^{-1} T^{-1} Q^2}{[(x_i - x_j)^2 + (y_i - y_j)^2 + (z_i - z_j)^2]^{1/2}}\right) \\ & \times \exp\left[-\left(\frac{m_i g + Q E}{k_B T}\right) z_i\right] d^3\mathbf{R}_i. \end{aligned} \quad (7)$$

2. Approximation

The presence of repulsive Coulomb interaction,

$$\sum_{j \neq i}^N \frac{-k_q k_B^{-1} T^{-1} Q^2}{[(x_i - x_j)^2 + (y_i - y_j)^2 + (z_i - z_j)^2]^{1/2}},$$

makes Eq. (7) difficult and this term must be approximated. The configuration depicted in Fig. 4 is referred for the analysis.

As the i th particle gets compressed in the direction of electric field, it experiences net electric field given by

$$\mathbf{E}_{\text{net}} = \mathbf{E}_{\text{el}} + \mathbf{E}_{\text{rep}},$$

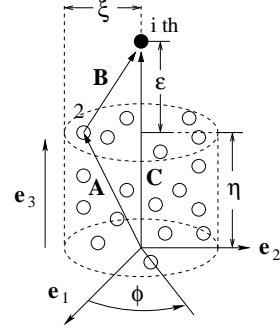


Figure 4: Particles are compressed in $-\mathbf{e}_3$ direction. The i th particle is the top most particle and all other particles are ahead of it in the direction of compression.

where \mathbf{E}_{el} is the electric field inside the chamber generated by external electrodes and \mathbf{E}_{R} is the electric field produced by all other particles inside the chamber. Because \mathbf{E}_{el} and \mathbf{E}_{rep} are oppositely directed, the magnitude $E_{\text{net}} \equiv \|\mathbf{E}_{\text{net}}\|$ is given by

$$E_{\text{net}} = E_{\text{el}} - E_{\text{rep}}. \quad (8)$$

To estimate E_{rep} , Fig. 4 is considered. The vectors \mathbf{A} , \mathbf{B} , and \mathbf{C} satisfy

$$\mathbf{B} = \mathbf{C} - \mathbf{A}. \quad (9)$$

In cylindrical coordinates, (ρ, ϕ, z) , \mathbf{A} and \mathbf{C} become

$$\begin{aligned} \mathbf{A} &= \rho_2 \cos(\phi_2) \mathbf{e}_1 + \rho_2 \sin(\phi_2) \mathbf{e}_2 + z_2 \mathbf{e}_3, \\ \mathbf{C} &= (\eta + \varepsilon) \mathbf{e}_3, \end{aligned}$$

where (ρ_2, ϕ_2, z_2) represents the cylindrical coordinates for particle labeled as 2 in Fig. 4. With \mathbf{A} and \mathbf{C} thus defined, Eq. (9) becomes

$$\mathbf{B} = -\rho_2 \cos(\phi_2) \mathbf{e}_1 - \rho_2 \sin(\phi_2) \mathbf{e}_2 + (\eta + \varepsilon - z_2) \mathbf{e}_3.$$

At \mathbf{C} , the electric field contributed from particle labeled as 2 is given by

$$\begin{aligned} \mathbf{E}_2 &= k_q Q \frac{\mathbf{B}}{\|\mathbf{B}\|^3} \\ &= \frac{k_q Q [-\rho_2 \cos \phi_2 \mathbf{e}_1 - \rho_2 \sin \phi_2 \mathbf{e}_2 + (\eta + \varepsilon - z_2) \mathbf{e}_3]}{[\rho_2^2 + (\eta + \varepsilon - z_2)^2]^{3/2}}. \end{aligned}$$

Because both gravitational and electrical forces are assumed to depend on z coordinate only, the \mathbf{e}_1 and \mathbf{e}_2 components of \mathbf{E}_2 average to zero to become

$$\mathbf{E}_2 = \frac{k_q Q (\eta + \varepsilon - z_2)}{[\rho_2^2 + (\eta + \varepsilon - z_2)^2]^{3/2}} \mathbf{e}_3.$$

All particles in the cylinder, not just the particle labeled as 2 in Fig. 4, contributes to form \mathbf{E}_{rep} . Hence,

$$\mathbf{E}_{\text{rep}} = k_q \sum_{j=1}^{N-1} \frac{Q (\eta + \varepsilon - z_j)}{[\rho_j^2 + (\eta + \varepsilon - z_j)^2]^{3/2}} \mathbf{e}_3, \quad (10)$$

where N is the number of charged particles in the chamber. For N sufficiently large, the coordinates ρ_j and z_j can be replaced by $\rho_j \rightarrow \rho$ and $z_j \rightarrow z$. In the continuum limit, the summation symbol gets replaced by

$$\sum_{j=1}^{N-1} \rightarrow \int_{z=0}^{\eta} \int_{\rho=0}^{\xi} \int_{\phi=0}^{2\pi} \rho d\phi d\rho dz$$

and the charge Q is replaced by

$$Q \rightarrow \frac{Q_{\text{tot}}}{\text{Volume}} = \frac{1}{2\pi\xi\eta} \sum_{j=1}^{N-1} Q = \frac{(N-1)Q}{2\pi\xi\eta},$$

where volume is that of cylinder illustrated in Fig. 4 and Q_{tot} is the total charge inside it. In the continuum limit then, where N is assumed to be sufficiently large, Eq. (10) can be approximated by

$$\begin{aligned} \mathbf{E}_{\text{rep}} &= \frac{k_q (N-1) Q}{2\pi\xi\eta} \\ &\times \int_{z=0}^{\eta} \int_{\rho=0}^{\xi} \int_{\phi=0}^{2\pi} \frac{(\eta + \varepsilon - z) \rho d\phi d\rho dz}{[\rho^2 + (\eta + \varepsilon - z)^2]^{3/2}} \mathbf{e}_3, \end{aligned}$$

which result, integrating over the ϕ , becomes

$$\begin{aligned} \mathbf{E}_{\text{rep}} &= \frac{k_q (N-1) Q}{\xi\eta} \\ &\times \int_{z=0}^{\eta} \int_{\rho=0}^{\xi} \frac{(\eta + \varepsilon - z) \rho d\rho dz}{[\rho^2 + (\eta + \varepsilon - z)^2]^{3/2}} \mathbf{e}_3. \end{aligned} \quad (11)$$

With the change of variable,

$$x = \rho^2 + (\eta + \varepsilon - z)^2, \quad dx = 2\rho d\rho,$$

the ρ integral in Eq. (11) becomes

$$\begin{aligned} \int \frac{(\eta + \varepsilon - z) \rho d\rho}{[\rho^2 + (\eta + \varepsilon - z)^2]^{3/2}} &\rightarrow \frac{(\eta + \varepsilon - z)}{2} \int \frac{dx}{x\sqrt{x}} \\ &= -\frac{(\eta + \varepsilon - z)}{\sqrt{x}}. \end{aligned}$$

With x reverted back to the original variable, the ρ integral becomes

$$\begin{aligned} &\int_{\rho=0}^{\xi} \frac{(\eta + \varepsilon - z) \rho d\rho}{[\rho^2 + (\eta + \varepsilon - z)^2]^{3/2}} \\ &= -\frac{(\eta + \varepsilon - z)}{\sqrt{\rho^2 + (\eta + \varepsilon - z)^2}} \Big|_0^{\xi} \\ &= 1 - \frac{(\eta + \varepsilon - z)}{\sqrt{\xi^2 + (\eta + \varepsilon - z)^2}}. \end{aligned}$$

Insertion of the result into Eq. (11) yields

$$\begin{aligned} \mathbf{E}_{\text{tot}} &\approx \frac{k_q (N-1) Q}{\xi} \mathbf{e}_3 - \frac{k_q (N-1) Q}{\xi\eta} \\ &\times \int_{z=0}^{\eta} \frac{\eta + \varepsilon - z}{\sqrt{\xi^2 + (\eta + \varepsilon - z)^2}} dz \mathbf{e}_3. \end{aligned} \quad (12)$$

With the change of variable,

$$y = \xi^2 + (\eta + \varepsilon - z)^2, \quad dy = -2(\eta + \varepsilon - z) dz,$$

the z integral in Eq. (12) becomes

$$\int \frac{\eta + \varepsilon - z}{\sqrt{\xi^2 + (\eta + \varepsilon - z)^2}} dz \rightarrow -\frac{1}{2} \int \frac{dy}{\sqrt{y}} = -\sqrt{y}.$$

With y reverted back to the original variable, the z integral becomes

$$\begin{aligned} &\int_{z=0}^{\eta} \frac{\eta + \varepsilon - z}{\sqrt{\xi^2 + (\eta + \varepsilon - z)^2}} dz \\ &= -\sqrt{\xi^2 + (\eta + \varepsilon - z)^2} \Big|_0^{\eta} \\ &= \sqrt{\xi^2 + (\eta + \varepsilon)^2} - \sqrt{\xi^2 + \varepsilon^2}. \end{aligned}$$

Insertion of the result into Eq. (12) gives the \mathbf{E}_{rep} ,

$$\begin{aligned} \mathbf{E}_{\text{rep}} &\approx \frac{k_q (N-1) Q}{\xi\eta} \\ &\times \left[\eta - \sqrt{\xi^2 + (\eta + \varepsilon)^2} + \sqrt{\xi^2 + \varepsilon^2} \right] \mathbf{e}_3. \end{aligned}$$

Since the z coordinate of the i th particle is given by

$$z_i = \eta + \varepsilon, \quad \eta = z_i - \varepsilon,$$

the expression for \mathbf{E}_{rep} may be rewritten in terms of z_i as

$$\begin{aligned} \mathbf{E}_{\text{rep}} &\approx k_q (N-1) Q \\ &\times \left[\frac{1}{\xi} - \frac{\sqrt{1 + z_i^2/\xi^2}}{z_i - \varepsilon} + \frac{\sqrt{1 + \varepsilon^2/\xi^2}}{z_i - \varepsilon} \right] \mathbf{e}_3. \end{aligned}$$

The parameter ε has been introduced for a mathematical convenience to assure that the i th particle is the upper most particle residing at the top surface of the compressed volume. Taking the limit $\varepsilon \rightarrow 0$, the previous expression for \mathbf{E}_{rep} becomes

$$\mathbf{E}_{\text{rep}} \approx k_q (N-1) Q \left(\frac{1}{z_i} + \frac{1}{\xi} - \sqrt{\frac{1}{z_i^2} + \frac{1}{\xi^2}} \right) \mathbf{e}_3. \quad (13)$$

Since z_i is the z coordinate for the i th particle, which is the particle residing at the top surface of the compressed volume in Fig. 4, the \mathbf{E}_{rep} defined in Eq. (13) represents

the Coulomb repulsion acting on the particle residing at the top surface of the compressed volume from all other ones within the compressed volume. Insertion of Eq. (13) into Eq. (8) gives

$$E_{\text{net}} \approx E_{\text{el}} - k_q (N-1) Q \left(\frac{1}{z_i} + \frac{1}{\xi} - \sqrt{\frac{1}{z_i^2} + \frac{1}{\xi^2}} \right).$$

The E_{net} in current form is only an approximation because the expression for \mathbf{E}_{rep} , Eq. (13), is an approximation. The equality can be made by replacing $Q \rightarrow Q_{\text{eff}}$, where Q_{eff} is the effective charge to be determined experimentally. With Q_{eff} , the expression for E_{net} becomes

$$E_{\text{net}} = E - k_q (N-1) Q_{\text{eff}} \left(\frac{1}{z_i} + \frac{1}{\xi} - \sqrt{\frac{1}{z_i^2} + \frac{1}{\xi^2}} \right), \quad (14)$$

where the subscript el of E_{el} has been dropped for convenience.

What is the implication of E_{net} ? The U_i of Eq. (3), which is the energy term assumed by the i th charged particle under the influence of external forces, can be rearranged in form as

$$U_i = \frac{\mathbf{p}_i^2}{2m_i} + m_i g z_i + Q \left\{ z_i E + \sum_{j \neq i}^N \frac{k_q Q}{\left[(x_i - x_j)^2 + (y_i - y_j)^2 + (z_i - z_j)^2 \right]^{1/2}} \right\}.$$

One notices that the term in the summation is the electric field contribution from the j th particle acting on the i th particle,

$$\|\mathbf{E}_{\text{rep},j}\| = \frac{k_q Q}{\left[(x_i - x_j)^2 + (y_i - y_j)^2 + (z_i - z_j)^2 \right]^{1/2}}.$$

Furthermore, one finds

$$E_{\text{rep}} \equiv \|\mathbf{E}_{\text{rep}}\| = \sum_{j \neq i}^N \|\mathbf{E}_{\text{rep},j}\|, \quad E = \|\mathbf{E}_{\text{el}}\|,$$

and U_i can be equivalently expressed as

$$U_i = \frac{\mathbf{p}_i^2}{2m_i} + m_i g z_i + Q (z_i E + E_{\text{rep}}).$$

Since $E_{\text{rep}} = E_{\text{el}} - E_{\text{net}}$, Eq. (8), the U_i becomes

$$U_i = \frac{\mathbf{p}_i^2}{2m_i} + m_i g z_i + Q (z_i + 1) E - Q E_{\text{net}}. \quad (15)$$

Insertion of Eq. (15) into Eq. (6) gives an alternate expression for probability density for finding particle with

its center of mass position in the ranges $(\mathbf{R}_i; d\mathbf{R}_i)$ and $(\mathbf{p}_i; d\mathbf{p}_i)$,

$$\begin{aligned} & P_s(\mathbf{R}_i, \mathbf{p}_i) d^3\mathbf{R}_i d^3\mathbf{p}_i \\ & \propto \exp \left[- \left(\frac{m_i g + Q E}{k_B T} \right) z_i + \frac{Q (E_{\text{net}} - E)}{k_B T} \right] d^3\mathbf{R}_i \\ & \times \exp \left(- \frac{\mathbf{p}_i^2}{2m_i k_B T} \right) d^3\mathbf{p}_i, \end{aligned} \quad (16)$$

which is different from the previous expression, Eq. (7), but now manageable. With Eq. (14) inserted for E_{net} , Eq. (16) becomes

$$\begin{aligned} & P_s(\mathbf{R}_i, \mathbf{p}_i) d^3\mathbf{R}_i d^3\mathbf{p}_i \\ & \propto \exp \left\{ \frac{k_q (1-N) Q Q_{\text{eff}}}{k_B T} \left(\frac{1}{z_i} + \frac{1}{\xi} - \sqrt{\frac{1}{z_i^2} + \frac{1}{\xi^2}} \right) \right. \\ & \left. - \left(\frac{m_i g + Q E}{k_B T} \right) z_i \right\} \exp \left(- \frac{\mathbf{p}_i^2}{2m_i k_B T} \right) d^3\mathbf{R}_i d^3\mathbf{p}_i, \end{aligned} \quad (17)$$

Equation (17) may be integrated over all possible x and y values lying within in the container and each components of the momentum may be integrated from $-\infty$ to ∞ ,

$$\begin{aligned} & P_s(z_i) dz_i \\ & \propto \int_{p_{ix}} \int_{p_{iy}} \int_{p_{iz}} \exp \left(- \frac{p_{ix}^2 + p_{iy}^2 + p_{iz}^2}{2m_i k_B T} \right) dp_{ix} dp_{iy} dp_{iz} \\ & \times \exp \left[\frac{k_q (1-N) Q Q_{\text{eff}}}{k_B T} \left(\frac{1}{z_i} + \frac{1}{\xi} - \sqrt{\frac{1}{z_i^2} + \frac{1}{\xi^2}} \right) \right. \\ & \left. - \left(\frac{m_i g + Q E}{k_B T} \right) z_i \right] dz_i \int_x \int_y dx_i dy_i. \end{aligned} \quad (18)$$

The double integral over x and y gives slice area of the chamber at $z = z'$, $0 < z' < L_z$,

$$\int_x \int_y dx_i dy_i = \pi \xi^2, \quad (19)$$

where ξ is the radius of cylindrical chamber depicted in Fig. 4. The momentum integrals are obtained utilizing the well known integral formula (author?) [17]

$$I(n) \equiv \int_0^\infty x^n \exp(-\alpha x^2) dx, \quad n \geq 0,$$

where solutions are given by

$$I(0) = \frac{1}{2} \sqrt{\frac{\pi}{\alpha}}, \quad I(1) = \frac{1}{2\alpha}, \quad I(2) = \frac{1}{4\alpha} \sqrt{\frac{\pi}{\alpha}}, \quad \text{etc.}$$

The momentum integrals become

$$\begin{aligned} & \int_{p_{ix}} \int_{p_{iy}} \int_{p_{iz}} \exp \left(- \frac{p_{ix}^2 + p_{iy}^2 + p_{iz}^2}{2m_i k_B T} \right) dp_{ix} dp_{iy} dp_{iz} \\ & = \frac{1}{8} (2\pi m_i k_B T)^{\frac{3}{2}}. \end{aligned} \quad (20)$$

With Eqs. (19) and (20), Eq. (18) becomes

$$P_s(z_i) dz_i \propto \frac{1}{8} \pi \xi^2 (2\pi m_i k_B T)^{\frac{3}{2}} \exp \left[\frac{k_q (1-N) Q Q_{\text{eff}}}{k_B T} \right] \times \left[\frac{1}{z_i} + \frac{1}{\xi} - \sqrt{\frac{1}{z_i^2} + \frac{1}{\xi^2}} - \left(\frac{m_i g + Q E}{k_B T} \right) z_i \right] dz_i.$$

With the following definitions,

$$\alpha = \frac{k_q (1-N) Q Q_{\text{eff}}}{k_B T}, \quad \beta = \frac{m_i g + Q E}{k_B T}, \quad (21)$$

the previous expression for $P_s(z_i) dz_i$ simplifies to

$$P_s(z_i) dz_i = \frac{1}{8} C \pi \xi^2 (2\pi m_i k_B T)^{\frac{3}{2}} \times \exp \left[\alpha \left(\frac{1}{z_i} + \frac{1}{\xi} - \sqrt{\frac{1}{z_i^2} + \frac{1}{\xi^2}} \right) - \beta z_i \right] dz_i, \quad (22)$$

where C is the constant of proportionality to be determined from the normalization condition, $\int_0^{L_z} P_s(z_i) dz_i = 1$. It can be shown

$$C = \frac{8}{\pi \xi^2} (2\pi m_i k_B T)^{-\frac{3}{2}} \times \left\{ \int_0^{L_z} \exp \left[\alpha \left(\frac{1}{x_i} + \frac{1}{\xi} - \sqrt{\frac{1}{x_i^2} + \frac{1}{\xi^2}} \right) - \beta x_i \right] dx_i \right\}^{-1}. \quad (23)$$

What can be said about Q_{eff} defined in α ? The effective Coulomb repulsion from the remaining $N-1$ charged particles inside the chamber acting on the i th charged particle, see Fig. 4, is proportional to

$$\mathcal{F}_{N-1} \propto (N-1) Q_{\text{eff}},$$

where Q_{eff} must be determined empirically from measurements. In principle, Q_{eff} takes into account the spatial configuration of the $N-1$ charged particles in the system because it effectively describes the system, which is illustrated in Fig. 4, in terms of the two body problem (see Fig. 5). Because the total charge in the imaginary cylinder must be conserved, it must be true that

$$0 < (N-1) Q_{\text{eff}} \leq (N-1) Q.$$

And, this implies the condition

$$0 < Q_{\text{eff}} \leq Q. \quad (24)$$

For describing the trend of volume compression involving charged particles, Eq. (24) provides the way to estimate Q_{eff} . Once Q_{eff} is defined, Eq. (22) may be plotted for the most probable height of the compressed volume,

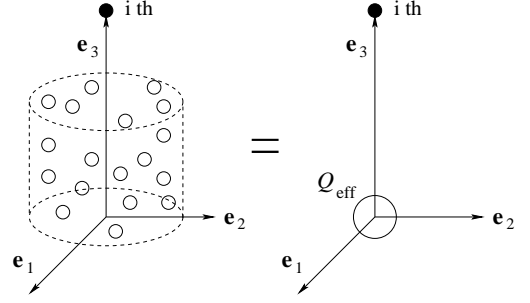


Figure 5: Transformation to the two body problem by introduction of effective charge for the particles inside the imaginary cylinder.

which volume contains the N charged particles in the system. That being said, combining Eqs. (22) and (23), the probability density for the most probable height of the compressed volume containing N charged particles becomes

$$P_s(z_i) dz_i = \left\{ \int_0^{L_z} \exp \left[\alpha \left(\frac{1}{x_i} + \frac{1}{\xi} - \sqrt{\frac{1}{x_i^2} + \frac{1}{\xi^2}} \right) - \beta x_i \right] dx_i \right\}^{-1} \times \exp \left[\alpha \left(\frac{1}{z_i} + \frac{1}{\xi} - \sqrt{\frac{1}{z_i^2} + \frac{1}{\xi^2}} \right) - \beta z_i \right] dz_i, \quad (25)$$

where α and β are defined in Eq. (21).

3. Result

Before plotting $P_s(z_i)$, I shall explicitly define the charge Q , particle mass m , and the electric field magnitude E .

In nature, the charge is quantized and, therefore, it is convenient to express Q in terms of the charge number n_e ,

$$Q_i = n_e q, \quad q = 1.602 \times 10^{-19} \text{ C}, \quad (26)$$

where q is the fundamental charge unit and $n_e = 0, 1, 2, 3, \dots$, is the number of electrons removed from the particle.

For the sake of simple analysis, the particles in the system are assumed to be spheres of identical radius. The mass of each particle would then be given by

$$m = \frac{4}{3} \pi r^3 \rho_m, \quad (27)$$

where r is the radius of sphere and ρ_m is the mass density.

Finally, the electric field generated in the chamber by control electrodes is

$$E \approx \frac{V_0}{L_e}, \quad (28)$$

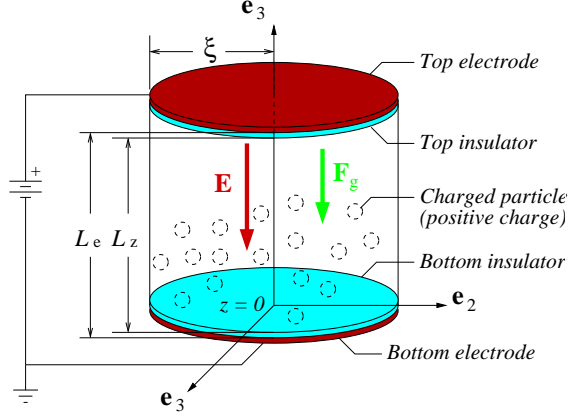


Figure 6: Configuration used to plot $P_s(z_i)$ defined in Eq. (25).

where V_0 is the voltage applied to the top electrode (the other electrode has been grounded). The approximation \approx in electric field comes about because the effects of passivation layers inside the chamber have been neglected for simplicity.

Having defined Q , m , and \mathbf{E} , the configuration illustrated in Fig. 6 is referred to plot $P_s(z_i)$, Eq. (25). The parameters for the configuration are given the following values:

$$\begin{cases} L_e = 100 \text{ um}, L_z = 90 \text{ um}, \xi = 50 \text{ um}, \\ \rho_m = 2.7 \text{ g cm}^{-3}, r = 50 \text{ nm}, \\ T = 42^\circ\text{C}, N = 1000, n_e = 15. \end{cases}$$

For the purpose of plotting $P_s(z_i)$ defined in Eq. (25), I shall assume, see Eq. (24),

$$Q_{\text{eff}} = 0.97Q,$$

where Q is defined in Eq. (26). The voltages of $V_0 = 0 \text{ V}$, 0.1 V , 0.2 V , 0.3 V , and 0.5 V are considered for the top electrode (the bottom electrode is grounded). With V_0 thus defined, the electric field generated inside chamber is given by Eq. (28). The gravity of $g = 9.8 \text{ m/s}^2 \geq 0$ was assumed inside the chamber. The directions for the electric field \mathbf{E} and the gravitational force \mathbf{F}_g are determined from Eqs. (4) and (5). Since both E and g are positive, according to the convention defined in Eqs. (4) and (5), the electric field \mathbf{E} and the gravitational force \mathbf{F}_g are both directed in $-\mathbf{e}_3$, which is the negative z axis. The $P_s(z_i)$ of Eq. (25) is computed numerically utilizing Simpson method for the integral (author?) [18]. The Simpson method routine was coded in **FORTRAN 90**. That being said, the results are summarized in Figs. 7 and 8, where the three smaller peaks of Fig. 7 are magnified and replotted in Fig. 8.

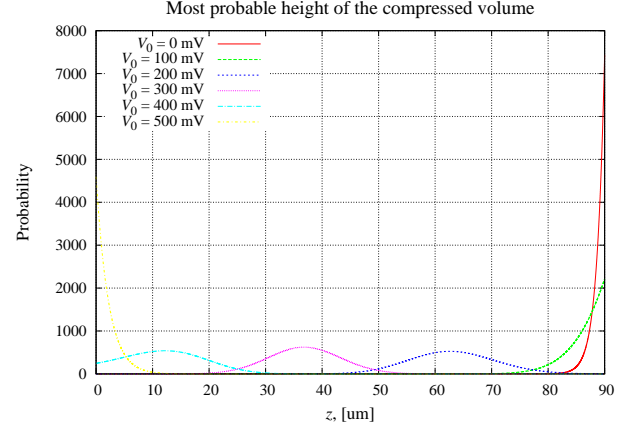


Figure 7: Most probable height of the compressed volume containing charged particles.

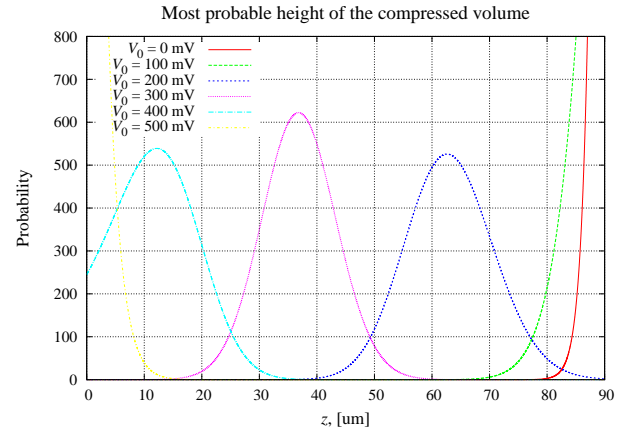


Figure 8: Illustrates the details three small peaks in Fig. 7. Each peak represents the most probable height of the compressed volume, where N charged particles are confined to.

At $V_0 = 0 \text{ V}$, that is, when there is no electric field inside the chamber other than the static fields from particles, the particles are distributed to occupy the entire volume of the chamber. This is indicated by the peak occurring at the physical height of the chamber, $h_c = z = L_z = 90 \text{ um}$.

At $V_0 = 0.2 \text{ V}$, an electric field of roughly $E \approx 2000 \text{ V m}^{-1}$ is generated inside the chamber. Because particles are positively charged, they are compressed in the direction of electric field, i.e., the $-z$ direction. This force, which induced particle volume compression, eventually gets counter balanced by the Coulomb repulsion and the compression ceases. For the case where control electrode is held at $V_0 = 0.2 \text{ V}$, the compression ceases at roughly $h_c = z \approx 63 \text{ um}$ (see Fig. 8) and this marks the most probable height of the compressed volume for the case. Finally, with $V_0 = 0.5 \text{ V}$ applied to the control electrode, the compressed volume state is reached where all particles are cluttered near the floor of the chamber,

thereby resulting in very high particle density, as illustrated in Fig. 7.

If charged particles are to be useful for any display applications, the charged particle system must be insensitive to gravitational effects, if not negligible. The effect of gravity on the most probable height for the compressed volume has been investigated by reversing the direction of gravity (but, keeping all other conditions unchanged) in Fig. 8. The case where $V_0 = 0.2$ V was selected for comparison. The result is shown in Fig. 9, where it shows that the most probable height for the compressed volume is only negligibly affected by the gravity.

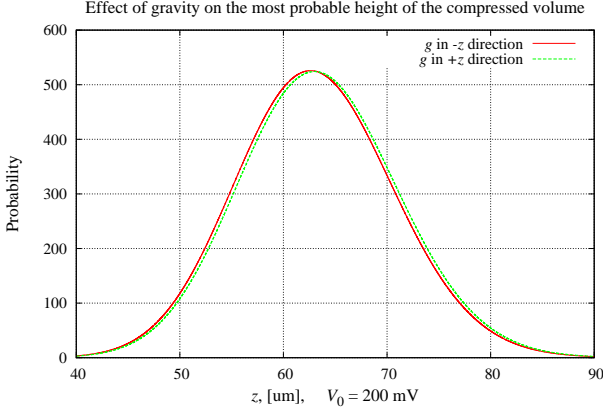


Figure 9: Gravity has negligible effect on most probable height of the compressed volume.

The influence of cylinder radius ξ on the most probable height for the compressed volume has also been investigated. Again, the case of $V_0 = 0.2$ V was selected from Fig. 8 for comparison by considering $\xi = 50$ um, 60 um, and 70 um. All other conditions were kept unmodified. The result, Fig. 10, reveals a decrease in height for the most probable compressed volume with increasing ξ as expected.

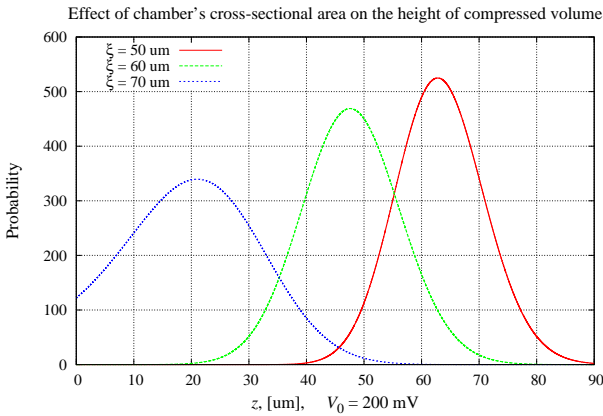


Figure 10: The height for the compressed volume decreases as the radius of cylinder increases.

D. Transmission intensity

The intensity of light transmitted through a medium filled with charged particles goes like, Eq. (2),

$$I \propto \exp(-\sigma_N),$$

where σ_N is the average number of particles per unit cross-sectional area. Because σ_N increases with decreased h_c , i.e., the height of the compressed particle volume schematically illustrated in Fig. 2, the two quantities are inversely related,

$$\sigma_N \propto \frac{1}{h_c},$$

and the intensity of light transmitted through a medium filled with charged particles follows as

$$I \propto \exp\left(-\frac{1}{h_c}\right). \quad (29)$$

The parameter h_c can be controlled by voltages applied to the control electrodes and this is demonstrated in Fig. 8. In principle, h_c can be varied continuously. This implies the intensity of light out of optical shutter can be varied continuously; and, this, in turn, implies the continuous grayscale levels for the device.

This work is not the first kind to address potential applications with charged particles. Szirmai experimented with alumina powders to study electrosuspension as early as 1990's?]. In Szirmai's experiment, alumina powder of 3 um in diameter was placed inside an electrically insulating cylindrical vessel, which is similar in configuration with Fig. 6. The initial charging of alumina powder was done by a process of field emission, which can be achieved by applying high voltage to the control electrodes[20]. Szirmai, however, does not quantitatively address the compression states of volume containing charged particles in terms of the design parameters, as his motive was not in discussing possible applications of charged particles for displays. In his experiment, the control electrodes, in principle, could be supplied with whatever high voltages required by it to do the job; therefore, the quantitative understanding of how design parameters, such as L_e , L_z , ξ , ρ_m , r , T , N , n_e , V_0 , and $Q_{\text{eff}} \propto Q$, enter into the picture of particle volume compression never was an issue.

The competition has always been fierce and it will always remain so among different display manufacturers. In the near future, when paper-like displays become dominant, the most important deciding factor to who stays in and goes out of business would be determined by the power efficiency of their products. That being said, a low operation voltage for the control electrodes is crucial for all E-paper technologies and the proposed device based on charged particles is no exception. The light intensity out of each sub-pixel based on proposed charged particle display technology varies as illustrated in Eq. (29), where

h_c is the most probable compression height corresponding to the voltage difference of V_0 applied to the control electrodes, see Fig. 7. With the V_0 restricted to certain range, say $0 \text{ V} \leq V_0 \leq 1 \text{ V}$, one cannot arbitrarily choose the other parameters which constitute the design parameters, i.e., L_e , L_z , ξ , ρ_m , r , T , N , n_e , and Q . For example, if too many electrons are removed from each of the aluminum particles, i.e., n_e , the voltage of $V_0 = 1 \text{ V}$ applied to one of the control electrodes (the other grounded) may not be sufficient enough to overcome the Coulomb repulsion between particles and compress the particle volume to a level where dark state is reached, assuming $V_0 = 0 \text{ V}$ defines the brightest state. On the other end, if too many charged particles are present in a chamber, i.e., the particle number N , the brightest state achieved by setting $V_0 = 0 \text{ V}$ for the control electrode may be too dark. The quantitative description of the height h_c of the compressed particle volume in terms of the so called “design parameters” thru the expression $P_s(z_i)$, Eq. (25), enables the design of particle based display with potential to generate continuous grayscale.

III. CONCLUDING REMARKS

The pioneering work by Szirmai, Hattori et al., and others have exposed the potential applications with charged particles. Utilizing charged particles in display technologies, however, requires a quantitative understanding of how design parameters, such as L_e , L_z , ξ , ρ_m , r , T , N , n_e , V_0 , and $Q_{\text{eff}} \propto Q$, enter into particle volume compression. In this work, an expression for the compressed state, which incorporates the design parameters, has been presented. The result should find its role in the development of displays based on charged particles.

IV. ACKNOWLEDGMENTS

The author acknowledges the support for this work provided by Samsung Electronics, Ltd.

-
- [1] I. Ota, “Electrophoretic Display Device,” U.S. Patent 3669106 (1972).
 - [2] N. Sheridan, “Twisting ball panel display,” U.S. Patent 4126854 (1978).
 - [3] J. Jacobson and H. Yoshizawa, “Heterogeneous display elements and methods for their fabrication,” U.S. Patent 6241921 (2001).
 - [4] J. Ding, C. Liao, S. Jeng, Y. Chen, and C. Lu, “Transflective electrophoretic display device,” U.S. Patent 20060087490 (2006).
 - [5] H. Mizuno, “Electrophoretic display apparatus,” U.S. Patent 7023609 (2006).
 - [6] H. Matsuda, “Display apparatus,” U.S. Patent 20070109622 (2007).
 - [7] B. Comiskey, J. Albert, H. Yoshizawa, and J. Jacobson, “An Electrophoretic Ink for All-Printed Reflective Electronic Displays,” *Nature* **394**, 253-255 (1998).
 - [8] T. Whiteside, M. Walls, R. Paolini, S. Sohn, H. Gates, M. McCreary, and J. Jacobson, “Towards Video-rate Microencapsulated Dual-Particle Electrophoretic Displays,” *SID Symposium Digest*, **35**, pp. 133-135 (2004).
 - [9] T. Kosc, “Particle display technologies become E-paper,” *Optics and Photonics News*, **16**(2), pp. 18-23 (2005).
 - [10] R. Sakurai, H. Hiraoka, T. Kobayashi, H. Yamazaki, and H. Kitano, “Image display panel and image display device,” U.S. Patent 0174854 (2008).
 - [11] R. Hattori, S. Yamada, Y. Masuda, and N. Nihei, “A novel bistable reflective display using quick-response liquid powder,” *J. Soc. Inf. Display*, **12** (1), pp. 75-80 (2004).
 - [12] R. Hattori, S. Yamada, Y. Masuda, N. Nihei, and R. Sakurai, “A quick-response liquid-powder display (QR-LPD®) with plastic substrate,” *J. Soc. Inf. Display*, **12** (4), pp. 405-409 (2004).
 - [13] R. Hattori, S. Yamada, Y. Masuda, N. Nihei, and R. Sakurai, “10.3: Distinguished Paper: Ultra Thin and Flexible Paper-Like Display using QR-LPD® Technology,” *SID Symposium Digest*, **35**, pp. 136-139 (2004).
 - [14] S. Kwon, S. Lee, W. Cho, B. Ryu, and M. Song, “62.4: Flexible Paper-Like Display Using Charged Polymer Particles” *SID Symposium Digest*, **37**, pp. 1838-1840 (2006).
 - [15] S. Johnson, *Stephen Johnson on Digital Photography* (O'Reilly Media, 2006).
 - [16] C. Bohren and D. Huffman, *Absorption and Scattering of Light by Small Particles* (John Wiley & Sons, New York, USA, 1998).
 - [17] F. Reif, *Fundamentals of statistical and thermal physics* (McGraw-Hill, New York, 1965).
 - [18] G. Thomas and R. Finney, *Calculus and analytic geometry*, 7th Ed, (Addison-Wesley, USA, 1988).
 - [19] S. Szirmai, “Charge transfer within electrostatic powder suspensions,” in *Industry Applications Conference, 2000. Conference Record of the 2000 IEEE*, (Rome, Italy, 2000), Vol. 2, pp. 851-857.
 - [20] Field emission is the phenomenon in which electrons get emitted from the surface of host material, such as nanoparticles, due to the presence of high electric fields.